

MET O 11 TECHNICAL NOTE NO. 167

A STRATIFORM CONDENSATION SCHEME FOR THE UKMO MESOSCALE MODEL

N A Machin

Met O 11 (Forecasting Research Branch),  
Meteorological Office,  
London Road,  
Bracknell,  
Berkshire,  
RG12 2SZ,  
England.

March 1983

N.B. This paper has not been published. Permission to quote from it must be obtained from the Assistant Director of the above Meteorological Office Branch.

JB

A STRATIFORM CONDENSATION SCHEME FOR THE UKMO MESOSCALE MODEL

1. Introduction

The effects of water vapour and its transition to and from the liquid state have often been ignored in numerical models of the planetary boundary layer. Not only would the inclusion of these processes be useful for the operational forecasting of cloudiness and precipitation but also important since the possible dynamical effects are quite large. For example, at a height of 1500 m, condensation of only 1% of the saturated humidity mixing ratio would release around  $100 \text{ J kg}^{-1}$  of energy, equivalent to a temperature increase of 0.1K or an increase in velocity from zero to  $14 \text{ ms}^{-1}$ . Although latent heat is normally realised as potential rather than kinetic energy, it is clear that it is an important energy source/sink and should be treated as accurately as possible in any numerical weather prediction model.

Carpenter (1979) has described a current version of the dry, non-hydrostatic mesoscale forecast model formulated by Tapp and White (1976). The model has a uniform horizontal grid with a resolution typically of 10 km, and variable spacing of terrain-following levels in the vertical. The experimental version of the model covers England and Wales and has 10 levels up to 4 km. A simple grid-scale moisture transport scheme which enables latent heat release during the condensation of water vapour to be included in the model was implemented some time ago. Preliminary results were encouraging and suggested that the process could form the basis of a more complete mesoscale stratiform (i.e. non-convective) condensation scheme which includes cloud water mixing ratio as an explicit prognostic variable of the model. Section 2 describes the formulation of such a scheme in which the microphysics of the various processes involved are based on parametrizations proposed by Sundqvist (1978) and successfully tested by him in a version of the ECMWF global grid point forecast model (Sundqvist, 1981). Implementation of the scheme in the mesoscale model is described in Section 3, and some preliminary results presented in Section 4.

Before the mesoscale model is available for operational use much development work is required on the input of initial data. For example, stratiform cloud would rapidly dissipate if simply inserted in regions of descent or low humidity. Section 5 describes a first experiment with the scheme to assess methods of forcing self-sustaining cloud systems into initial mesoscale fields. A list of notation is given in Appendix A.

## 2. Formulation

### a. Basic Assumptions

The scheme incorporates the hydrological cycle shown in Figure 1 into the model. To avoid the ambiguity evident in some literature, the opportunity is taken here to define autoconversion to be the spontaneous growth of cloud droplets via the ice phase (the Bergeron process), coalescence to be the growth of cloud droplets falling relative to, and colliding with, smaller droplets, and accretion to be the collection of cloud droplets by falling rain drops. Note that no account of the ice phase is explicitly included in the scheme at present. The various processes that are represented are based on the following assumptions.

- i. No condensation of water vapour takes place until the air becomes saturated on the grid scale. Refinement to sub-grid-scale condensation in which stratiform cloud is allowed to occupy only part of a grid-box was considered to be over elaborate in this model with a typical grid spacing of  $10 \times 10 \times \frac{1}{2}$  km.
- ii. Condensation of water vapour takes place at a sufficient rate to keep the air exactly saturated whenever super-saturation would otherwise occur.
- iii. Evaporation of any cloud droplets takes place at a sufficient rate to keep the air exactly saturated whenever sub-saturation would otherwise occur.

iv. Cloud droplets are advected with the grid scale wind velocity plus an average terminal fall velocity which depends only on the cloud water mixing ratio.

v. Growth of cloud droplets into rain drops (involving no change of state) depends only on the cloud water mixing ratio (for the auto-conversion and coalescence processes) and integrated precipitation rate falling from above (for the accretion process).

vi. Rain drops fall immediately and, subject to evaporation into any sub-saturated lower layers, are interpreted as surface precipitation over a single timestep.

vii. Evaporation of falling rain drops depends only on the integrated precipitation rate and ambient relative humidity.

The more detailed assumptions used in deriving the parametric relations are described in Sundqvist (1981).

Note that at present there is no link via surface wetness between surface precipitation and turbulent flux of water vapour from the surface. Since no account is taken of the effect of clouds on radiation at present, any interaction between the scheme and the rest of the model can occur only via latent heating during the condensation of water vapour, or the latent cooling during the evaporation of cloud water or falling raindrops.

b. Equations and Parametrizations

In addition to the momentum equation, the mass continuity equation and the thermodynamic equation, a further two prognostic equations, for humidity mixing ratio ( $q$ ) and cloud water mixing ratio ( $m$ ), are now included in the model.

$$\frac{\partial q}{\partial t} = A_r + E_r - P_r + F_r \quad (1)$$

The terms on the rhs represent the local rates of change of humidity mixing ratio due to advection of water vapour ( $A_r$ ), evaporation of falling raindrops ( $E_r$ ), condensation of water vapour (or evaporation of cloud droplets) ( $P_r$ ) and diffusion of water vapour ( $F_r$ ).

$$\frac{\partial m}{\partial t} = A_r + P_r - E_r + F_r \quad (2)$$

The new terms represent the local rates of change of cloud water mixing ratio due to advection of cloud droplets ( $A_c$ ), growth to rain drops ( $P_c$ ), and settling of cloud droplets ( $F_c$ ).

Consequently the rhs of the thermodynamic equation now includes a latent heating term,  $L_s$ .

$$\frac{\partial \theta}{\partial t} = A_s + F_s + L_s \quad (3)$$

$A_s$  and  $F_s$  are the existing local rates of change of potential temperature due to advection and diffusion (plus any convective adjustment) of heat. The effect of water vapour and cloud droplets on the equations of motion are considered to be negligible in this stratiform condensation scheme.

i. Condensation of water vapour term  $P_r$

Condensation is implemented diagnostically so that preliminary values of temperature and humidity mixing ratio are predicted at grid points neglecting any condensation, giving values  $T^*$  and  $q^*$ . A test is then made for saturation with respect to liquid water on the grid-scale by comparing  $q^*$  with the relevant saturation mixing ratio  $q_s(T^*)$ .

If the air is super-saturated,  $q > q_s(T^*)$ , there is assumed to be just enough condensation to bring the air to exact saturation, with corresponding latent heating.

However, if the air is sub-saturated,  $q < q_s(T^*)$ , and there is cloud water present,  $m > 0$ , then just enough is assumed to evaporate to

bring the air to exact saturation, provided there is enough cloud water available, and there is corresponding latent cooling. In either case the preliminary values of temperature and humidity mixing ratio are changed.

$$q = q^* - \Delta q \quad (4)$$

$$T = T^* + \Delta T \quad (5)$$

Since  $q_s \ll 1$  it can be assumed that the heat capacity of the remaining water vapour is negligible compared with that of the dry air. Hence the heat conservation equation in finite difference form can be written

$$\Delta T = L/c_p \left\{ q^* - q_s(T^* + \Delta T) \right\} \quad (6)$$

The Clausius-Clapeyron equation specifies the variation of saturation vapour pressure with temperature thus

$$de_s/dT = Ee_s/RT^2 \quad (7)$$

Since  $e_s \ll p$  we can write  $q_s \approx Ee_s/p$  so that the Clausius-Clapeyron equation in finite difference form can be written

$$\frac{q_s(T^* + \Delta T) - q_s(T^*)}{\Delta T} = \frac{E q_s(T^*) L}{RT^2} \quad (8)$$

Substituting for  $\Delta T$  from (6) into (8) yields the following after some rearrangement

$$q^* - q_s(T^* + \Delta T) = \left\{ \frac{1}{1 + \frac{E q_s(T^*) L^2}{c_p R T^2}} \right\} [q^* - q_s(T^*)], \quad (9)$$

which is more simply written thus

$$\Delta q = \left\{ \frac{1}{1 + \alpha} \right\} [q^* - q_s(T^*)] \quad (10)$$

Clearly the  $\alpha$  term arises so that changes in temperature and humidity mixing ratio keep pace with each other during latent heat release. It typically has a value greater than unity near the surface and only becomes small ( $\approx 0.1$ ) above about 9 km in the standard atmosphere.

If the preliminary values of temperature and humidity mixing ratio are predicted over a leapfrog timestep then the rate of change of humidity mixing ratio due to the condensation of water vapour (or the evaporation of cloud droplets) is given by

$$P = 1/2\delta t \left\{ \frac{1}{1+\alpha} \right\} [q^* - q_s(T^*)] \quad (11)$$

ii. Diffusion of water vapour term  $F_r$

At present this term includes only the boundary layer turbulence term

$$F_r = d/d\eta (-\overline{\eta' q'}) \quad (12)$$

where the downward turbulent flux of moisture is given by K-theory

$$\overline{-\eta' q'} = K_H d\eta \quad (13)$$

except close to the surface where it is given by the bulk aerodynamic formula

$$\overline{-\eta' q'}_{surf} = |V| C_H (q_{air}^{surf} - q_s^{surf}) \quad (14)$$

However  $q_{surf}$  is not generally known, so following Carpenter (1977) we say that over a dry surface the evaporation must be supplied by transpiration through the vegetation and this is described by a resistance formula

$$\overline{-\eta' q'}_{surf} = -\frac{q_{surf} - q_s^{surf}}{r} \quad (15)$$

Substitution for  $q_{surf}$  from (15) into (14) and some rearrangement yields

$$\overline{-\eta' q'}_{surf} = \frac{|V| C_H}{1+r|V|C_H} (q_{air}^{surf} - q_s^{surf}) \quad (16)$$

Over a water surface or if dew is forming ( $q^{air} > q^{swf}$ ), surface resistance to evapotranspiration  $r$  is set to zero.

Horizontal moisture diffusion is neglected at present.

iii. Settling of cloud water term  $F_t$

This is simply defined as

$$F_t = -\partial/\partial\eta (\dot{H}_m) . \quad (17)$$

The average terminal fall velocity of the cloud droplets,  $\dot{H}$ , is assumed to depend only on cloud water mixing ratio using the parametrization derived by Sundqvist (1981). The numerical value of his scaling velocity  $\tilde{c}_H$  is approximately transformed from a  $\sigma$  to a  $\eta$  vertical coordinate system, via the hydrostatic relation, for this scheme.

$$\dot{H} = \tilde{c}_H m^{2/3} \quad (18)$$

Using a value of  $\tilde{c}_H = 10 \text{ ms}^{-1}$ , cloud droplets with a typical mixing ratio of  $4 \times 10^{-4} \text{ (kgkg}^{-1}\text{)}$  will have an average terminal fall velocity of  $5 \text{ cms}^{-1}$ . Substituting for  $\dot{H}$  from (18) into (17) yields

$$F_t = -\tilde{c}_H \partial/\partial\eta (m^{5/3}) . \quad (19)$$

Horizontal and vertical diffusion of cloud droplets is neglected.

iv. Growth of raindrops term  $P_t$

The proportion of cloud droplets which grow and fall out as precipitation is assumed to depend on the cloud water mixing ratio, using essentially the parametrization devised by Sundqvist (1978). A simple accretion term  $\tilde{c}_R P_R$  (where  $P_R$  is the integrated precipitation rate reaching this level - see Appendix B) has been added for the present scheme.

$$P_t = \left[ \tilde{c}_T + \tilde{c}_R P_R \right] \left[ 1 - \exp \left\{ - \left( m / \tilde{c}_m \right)^2 \right\} \right] m \quad (20)$$

Note that  $\left\{ \left[ \tilde{c}_p + \tilde{c}_a P_R \right] \left[ 1 - \exp \left\{ - \left( m / \tilde{c}_m \right)^2 \right\} \right] \right\}^{-1}$  can be thought of as the typical conversion time of cloud droplets to rain drops, with limiting time  $\left[ \tilde{c}_p + \tilde{c}_a P_R \right]^{-1}$ . Choosing  $\tilde{c}_p = 10^{-4} \text{ s}^{-1}$  ( $10^4 \text{ s} = 2.8 \text{ hours}$ ) and  $\tilde{c}_a = 1.0 \text{ m}^2 \text{ kg}^{-1}$ , the rate of conversion is doubled by accretion with a precipitation rate of  $10^{-4} \text{ kg m}^{-2} \text{ s}^{-1}$  ( $\approx 0.4 \text{ mm hr}^{-1}$ ).

In an investigation of various stratiform condensation schemes, Riddaway (1978) modifies the parametrization for autoconversion and coalescence (which he simply calls autoconversion) used by Jonas (1976) so that it is similar to expression (20) without the accretion term, but chooses  $\tilde{c}_p$  (his  $1/\tau$ ) =  $10^{-3} \text{ s}^{-1}$  ( $10^3 \text{ s} = 17 \text{ mins}$ ). This seems to be much too rapid a conversion time for these processes alone and probably explains why his results showed that he could ignore accretion (which he calls collection). Note that using the above values for  $\tilde{c}_p$  and  $\tilde{c}_a$  then  $\left[ \tilde{c}_p + \tilde{c}_a P_R \right] = 10^{-3} \text{ s}^{-1}$  when  $P_R = 9 \times 10^{-4} \text{ kg m}^{-2} \text{ s}^{-1}$  ( $\approx 3 \text{ mm hr}^{-1}$ ) which corresponds to moderate rain.

The parameter  $\tilde{c}_m$  represents the value of cloud water mixing ratio at which a cloud can be considered to be in a well developed precipitating stage. Choosing  $\tilde{c}_m = 5 \times 10^{-4}$ , a value of  $m \lesssim 2.5 \times 10^{-4}$  produces such long conversion times ( $\approx 13 \text{ hours}$  with negligible accretion) that the cloud is effectively non-precipitating.

#### v. Evaporation of rain drops term $E_r$

The rate at which falling rain drops are evaporated back to water vapour is assumed to depend on the ambient sub-saturation and the integrated precipitation rate from above ( $P_L$ ), (see Appendix B), following Sundqvist (1981).

$$E_r = \tilde{c}_E \left\{ 1 - \frac{q^*}{q_s(T_r)} \right\} P_L^{1/2} \quad (21)$$

Choosing  $\tilde{C}_E = 2 \times 10^{-5}$  (SI) a precipitation rate of  $10^{-4} \text{ kgm}^{-2}\text{s}^{-1}$  ( $\approx 0.4 \text{ mm hr}^{-1}$ ) falling through an ambient relative humidity of 75% will be reduced by 25% whereas precipitation of less than  $5 \times 10^{-6} \text{ kgm}^{-2}\text{s}^{-1}$  will be completely evaporated.

vi. Latent heating term  $L_s$

Following the assumption used for expression (6) we can write

$$\left(\frac{\partial T}{\partial t}\right)_{\text{latent}} = -L/c_p \left\{ \left(\frac{\partial q}{\partial t}\right)_{\text{evap}} + \left(\frac{\partial q}{\partial t}\right)_{\text{cond}} \right\} \quad (22)$$

From a definition of Exner pressure  $P = T/\theta$  we have at constant pressure

$$\frac{\partial \theta}{\partial t} = 1/P \frac{\partial T}{\partial t} \quad (23)$$

Hence (22) becomes

$$\left(\frac{\partial \theta}{\partial t}\right)_{\text{latent}} = -L/c_p P \left\{ \left(\frac{\partial q}{\partial t}\right)_{\text{evap}} + \left(\frac{\partial q}{\partial t}\right)_{\text{cond}} \right\} \quad (24)$$

Using the notation of expressions (1) and (3) we simply have

$$L_s = -L/c_p P \left\{ E_r - P_r \right\} \quad (25)$$

vii. Advection terms  $A_r, A_t$

For completeness the new advection terms are also set down here

$$A_r = u \frac{\partial q}{\partial x} + v \frac{\partial q}{\partial y} + w \frac{\partial q}{\partial \eta} \quad (26)$$

$$A_t = u \frac{\partial m}{\partial x} + v \frac{\partial m}{\partial y} + w \frac{\partial m}{\partial \eta} \quad (27)$$

3. Implementation

In common with the existing model equations, the finite difference approximations to the water vapour and cloud water equations are centred in both space and time. The advection and vertical diffusion of water vapour are calculated exactly as those of the existing model variables, with the same boundary conditions.

$$\left(\frac{dq}{dt}\right)_b^t = \left(\frac{dq}{dt}\right)_i^{t-\delta t}$$

$$\left(\frac{dq}{dt}\right)_{surf}^t = 0$$

The condensation scheme is applied only at interior points, so that although the advection of cloud water is calculated similarly, the boundaries remain cloudless at present.

$$m_b^t = 0$$

The forecast procedure including the new moisture variables can then be summarised as follows:

- a. From terms calculated during the previous timestep, update the existing model variables, plus  $q$  and  $m$ , from time level  $t-2\delta t$  to  $t$ .
- b. Calculate the terms for updating the existing model variables from time level  $t-\delta t$  to  $t+\delta t$  as before, including the advection and diffusion of heat ( $A_s$  and  $F_s$ ).
- c. Ignoring the accretion process, calculate the growth (by autoconversion and coalescence) of rain drops ( $P_t'$ ) using  $m^t$  in expression (20).
- d. Calculate the advection and diffusion of water vapour ( $A_r$  and  $F_r$ ) using  $q^t$  and  $q^{t-\delta t}$ .
- e. Ignoring condensation, calculate a preliminary value  $\theta_*$  from  $\theta^{t-\delta t}$  using  $A_s$  and  $F_s$ . Then  $T_* = \theta_* P^t$ .
- f. Ignoring condensation, calculate a preliminary value  $q_*$  from  $q^{t-\delta t}$  using  $A_r$  and  $F_r$ .
- g. Calculate  $e_s(T_*)$  using a sixth order polynomial in  $T_*$ . Then  $q_s(T_*) = E_{es}(T_*) / p^{t-es}(T_*)$ .
- h. Calculate the condensation of water vapour ( $P_r$ ) using  $T_*$ ,  $q_*$  and  $q_s(T_*)$  in expression (11).

- i. Integrate the precipitation down through the model levels, incorporating the accretion process of expression (20) to give the full precipitation term ( $P_t$ ). Thus calculate the evaporation of rain drops term ( $E_r$ ) of expression (21). Since the procedure is not completely straightforward a detailed description is given in Appendix B.
- j. From the difference between condensation of water vapour ( $P_c$ ) and evaporation of rain drops ( $E_r$ ) calculate the latent heat ( $L_s$ ) as expression (25), and add it to the remainder of the diabatic term in the thermodynamic equation.
- k. Calculate the advection of cloud water ( $A_c$ ) using  $m^t$  and  $m^{t-\delta t}$ .
- l. Calculate the fall velocity of cloud water ( $F_c$ ) using  $m^t$  in equation (19).
- m. From terms calculated this timestep update existing model variables plus  $q$  and  $m$  from time level  $t-\delta t$  to  $t+\delta t$ .

Thus the process is repeated each timestep.

Time smoothing of  $q$  and  $m$  is carried out exactly as for the existing model variables. In order to avoid small negative humidity mixing ratio values, which may be caused by truncation errors of the finite difference scheme, if  $q^{t+\delta t}$  is found to be negative it is simply set to zero. Similarly, to avoid wasteful calculations with negligibly small cloud water mixing ratios, values of  $m^{t+\delta t} < 10^{-8}$  are set to zero at the end of each timestep.

#### 4. Preliminary Results

In the absence of humidity and cloud water initialisations at present, the scheme has been tested on an arbitrarily chosen dry initialisation in which the humidity mixing ratio was set to  $5 \times 10^{-3}$  everywhere (but was previously used only at the first level in the calculation of the surface heat balance). The new cloud water field was set to zero initially.

The forecast/model incorporating the new condensation scheme was initially run for two 'moisture initialising' timesteps during which all condensate was removed from the model with no latent heat release. For the chosen data (1800 GMT 2 January 1978) this left the model just saturated above about 500 m AMSL. The 'cloudy' forecast was then continued for 120 one minute timesteps. A 'moist' forecast in which any condensate is removed immediately from the model, and a 'dry' forecast in which the latent heat release is set to zero every timestep, were also run for comparison.

In the cloudy forecast stratiform cloud develops during the first 35 timesteps or so and thereafter is maintained relatively unchanged over the highest orography (for example Figure 3). Maximum cloud water mixing ratios are over  $5 \times 10^{-4}$  just above the cloud base, with half that value being typical of most of the cloud. Although constrained by the top level of the experimental model, the cloud is little affected since forcing is essentially orographic in this case. Indeed isolated precipitation rates of up to  $0.5 \text{ mm hr}^{-1}$  (corresponding to light rain) and more generally 0.1 to  $0.2 \text{ mm hr}^{-1}$  (light to moderate drizzle) are produced below densest cloud (Figure 2).

Comparison with the moist forecast (not shown) highlights the major deficiency of such a model in that 'cloud' or 'precipitation' is restricted to regions of condensation, since there is no transport of cloud water. In the forecast incorporating the new scheme, areas of heaviest precipitation occur around 30 km downwind of maximum condensation and the cloud is advected at least a further 30 km before being completely evaporated. Figure 5 contrasts cloud water budgets at the windward edge and 30 km downwind within the orographic cloud shown in Figure 3. On the windward edge condensation is being maintained in a region of strong ascent where water vapour is advected from lower levels with larger humidity mixing ratios, and cooling by adiabatic expansion is partially compensated for by the continuous latent heating, according to the saturated lapse rate. Once the cloud has developed this essentially balances the continuous advection of cloud free air at this edge, with the settling and precipitation terms at least an order of magnitude smaller.

In contrast, after the cloud has been advected 30 km downwind from the source region, a much weaker balance is set up. Slight descent is able to just maintain sub-saturation in this region so that the cloud slowly evaporates. Together with loss as rain drops, this essentially balances the weak advection of cloud droplets from the condensation region and the settling of cloud droplets from above.

The results of these changes in water state are shown in Figures 3 and 4. After 120 timesteps, potential temperature increases of more than  $1\frac{1}{2}$  K from those of the dry forecast develop in regions where greatest condensation is maintained. However, an area of up to 1K cooling relative to the dry forecast downwind of this region suggests that the process is not as straightforward as it first appears. If the warming is due solely to condensation, then as the cloud evaporates downwind, the air would simply be cooled back to its original potential temperature. Indeed in this case some liquid water is lost as precipitation so that the air should actually be warmer than in the dry forecast downwind of orography (i.e. the fohn effect). Further inspection of Figures 3 and 4 shows that there are substantial differences in vertical velocities between the cloudy and dry forecasts.

The dry forecast using these data shows a very large reduction and backing of the surface (actually 10 m above the surface) wind over windward slopes and an almost as large acceleration and veering down the lee slope. The resulting convergence and divergence forces very strong ascent and descent over orography in the dry forecast (Figure 4). Carpenter (1977) noted that the boundary layer parametrization used in this experiment was developed with the application to clear anticyclonic conditions in mind, so that it takes no account of moist processes. Consequently the latent heat released during condensation increases the apparent stability of the air just above windward slopes, reducing the vertical turbulent flux of momentum and consequently the effect of surface friction at 10 m. Conversely the evaporative cooling above the lee slope reduces the apparent stability and hence increases the effect of surface friction there. The result is therefore a smoother surface wind (Figure 2) and a substantial reduction in vertical velocities over orography in the cloudy forecast (Figure 3).

If processes were purely adiabatic with the potential temperature remaining constant following the motion (which is essentially the case in Figure 4) then a substantial reduction in vertical velocities alone would account for potential temperature differences similar to those shown in Figure 4. However it is clear from Figure 3 that the diabatic condensation and evaporation in the cloudy forecast have helped to reinforce the pattern since, following the motion, potential temperature increases (markedly) over windward slopes and decreases (less) over lee slopes.

##### 5. A cloud assimilation experiment

The first in a series of experiments to test possible techniques for assimilating cloud information into the mesoscale model with the stratiform condensation scheme was carried out using the same initial data as the forecast in Section 4. After the initial settling down period a large cloud free area in SE England was selected in which there were negligible vertical velocities, the atmosphere was stable and the relative humidity was around 85%. At grid points in an 85 km band aligned approximately normal to the wind flow, 1% super-saturation was forced between 210 m and 3600 m above the surface for 20 one minute timesteps.

Figure 6a shows a typical cross-section of cloud water mixing ratio and vertical velocity through the band at the end of the assimilation period. Except where it is affected by the top of this rather shallow experimental version of the model, cloud has formed only at those grid points where super-saturation was forced. The maximum cloud water mixing ratio of  $4 \times 10^{-4}$  just inside the leading edge of the band is not simply due to horizontal advection of cloud since droplets would be transported less than 20 km during the assimilation period. Rather, a slight increase in humidity mixing ratio and hence condensation, due to advection of water vapour at this edge gives maximum diabatic heating and induces ascent of over  $15 \text{ cms}^{-1}$ . Advection of water vapour from lower levels with larger humidity mixing

ratios and cooling by adiabatic expansion is then the important cloud building process there. Compensating descent of  $5 \text{ cms}^{-1}$  is induced outside both edges and more suprisingly within the centre of the cloud band itself.

After the assimilation period, the forecast was allowed to proceed without further interference. After 20 timesteps (Figure 6(b)), although the band has moved with the horizontal flow, its essential characteristics have been retained. The maximum cloud water mixing ratio inside the leading edge has been maintained, although ascent there has decayed to  $10 \text{ cms}^{-1}$ . The increased descent in the centre of the band has begun to divide the cloud as a second cloud water maximum forms inside the windward edge.

80 timesteps after the assimilation period (Figure 6(c)) the cloud has divided into two bands. Since the position of the leading edge of the cloud is determined more by the induced vertical circulation than by the horizontal advection of cloud droplets it is not surprising that this edge has travelled much more slowly than the wind speed at all levels. Thus cloud formed in the region of ascent is advected ahead of it and quickly evaporates in the descending air. The consequent diabatic cooling maintains the descent. Thus a circulation is set up and maintained by the horizontal wind, which continuously advects water vapour to the leading edge for condensation, and cloud water away from it for evaporation.

No such circulation is set up at the windward edge and it has travelled almost as quickly as the horizontal wind speed. Clearly the consequent reduction in cloud width to around 60 km has contributed to the growth of the cloud water mixing ratio maxima since there is a further slight decay in the vertical circulation.

It is clear that the experiment has been successful in assimilating a not unrealistic-looking cloud, and inducing a vertical circulation favourable for the maintainance of that cloud for at least 2 hours in an area which the model previously considered to be cloud free. Whether the behaviour of such a cloud system is realistic and/or desirable is another question and further experiments are being carried out.

## 6. Summary

The formulation and implementation of a stratiform condensation scheme for the mesoscale model is described, in which humidity and cloud water mixing ratio are prognostic variables of the model and the microphysical processes are parametrized. Important latent heat effects are thus included in the model.

A test forecast using artificial moisture data appears to give realistic cloud water budgets. However it is difficult to assess how far differences from a forecast without the scheme are due to the scheme, or to the inadequate boundary layer parametrization in the model at present. Further testing therefore awaits a realistic moisture initialisation and the implementation of the improved boundary layer parametrization at present under development.

A first attempt at assimilating cloud into the mesoscale model with the condensation scheme was successful in inserting a cloud and inducing a vertical circulation which maintained the cloud in a previously cloud free region for a substantial time after the assimilation ceased. Further experiments are planned to determine if a similar method should be used to assimilate cloud data into an operational version of the model.

## 7. Acknowledgement

Thanks are due to Dr B W Golding for useful ideas and helpful discussions.

## References

- Carpenter, K M                    1977    Surface exchanges in a mesoscale model of the atmosphere (unpublished) Met O 11 Tech. Note 96.
- 1979    An experimental forecast using a non-hydrostatic mesoscale model. Q J R Met. Soc., 105, 629-655.
- Jongs, P R                         1976    A revised parameterization of the condensation and precipitation processes for use in numerical forecasting models (unpublished) Met O 11 Tech. Note 67.
- Riddaway, R W                    1978    An investigation of various sub-grid-scale condensation schemes (unpublished) Met O 11 Tech. Note 122.
- Sundqvist, H                      1978    A parameterization scheme for non-convective condensation including prediction of cloud water content. Q J R Met. Soc., 104, 677-690.
- 1981    Prediction of stratiform clouds: Results from a 5-day forecast with a global model. Tellus, 33, 242-253.
- Tapp, M C and White, P W       1976    A non-hydrostatic mesoscale model. Q J R Met. Soc., 102, 277-296.

APPENDIX A

NOTATION

$P$	pressure	(Pa)
$T$	temperature	(K)
$\theta$	potential temperature (wrt $P_{ref}$ )	(K)
$q$	humidity mixing ratio	( $kgkg^{-1}$ )
$w$	cloud water mixing ratio	( $kgkg^{-1}$ )
$T_*, \theta_*, q_*$	predicted values of $T, \theta$ and $q$ ignoring condensation	
$\eta$	height above orography	(m)
$q_s$	saturation humidity mixing ratio	( $kgkg^{-1}$ )
$e_s$	saturation vapour pressure	(Pa)
$\Delta T, -\Delta q$	changes in $T$ and $q$ due to condensation	
$P_{ref}$	arbitrary reference pressure	(Pa)
$P = (P/P_{ref})^{R/c_p}$	Exner pressure	(dimensionless)
$\delta t$	length of model timestep	(s)
$ V $	horizontal wind speed	( $ms^{-1}$ )
$K_H$	eddy diffusivity of heat and moisture	( $m^2s^{-1}$ )
$C_H$	bulk heat transfer coefficient	(dimensionless)
$r$	surface resistance to evapotranspiration	( $sm^{-1}$ )
$C_p$	specific heat of dry air at constant pressure	( $1005 Jkg^{-1}K^{-1}$ )
$R$	gas constant for dry air	( $287 Jkg^{-1}K^{-1}$ )
$L$	latent heat of condensation	( $2.5 \times 10^6 Jkg^{-1}$ )
$\epsilon$	ratio of molecular weights of water and dry air	(0.622)
$\psi_b^t, \psi_i^t$	boundary and first interior values of $\psi$ at time level $t$	

The following quantities are the parameters of the stratiform condensation scheme.

- $\alpha$  scaling velocity for average terminal fall velocity of cloud droplets
- $\beta$  limiting time-scale for the rate of conversion of cloud droplets into rain drops by autoconversion and coalescence
- $\gamma$  time-scale parameter for the rate of conversion of cloud droplets into rain drops by accretion.
- $\delta$  characteristic value of cloud water mixing ratio around which a cloud reaches a fully precipitating stage.
- $\epsilon$  time-scale parameter for evaporation of falling rain drops.

The set of parameter values employed in the experiments was as follows.

- $\alpha = 10 \text{ ms}^{-1}$
- $\beta = 10^{-4} \text{ s}^{-1}$
- $\gamma = 1 \text{ m}^2 \text{ kg}^{-1}$
- $\delta = 5 \times 10^{-4}$
- $\epsilon = 2 \times 10^{-5} \text{ (SI)}$

APPENDIX B

Determination of Integrated Precipitation Rates

To be able to sum precipitation (and its evaporation) down through the model levels a conversion must be made from mixing ratio rates ( $kgkg^{-1}s^{-1}$ ) to areal density rates ( $kgm^{-2}s^{-1}$ ) to take into account variable layer thicknesses and densities. The following notation is used for the required areal density rates:

- $P_R(k)$  precipitation reaching level  $k$
- $P_G(k)$  precipitation generated at level  $k$
- $P_L(k)$  precipitation leaving level  $k$
- $E_v(k)$  evaporation at level  $k$

Since the top model level  $NZ$  is maintained cloudless we have

$$P_R(NZ-1) = 0$$

So that there can be no accretion at level  $NZ-1$  (see Section 3c.)

$$P_G(NZ-1) = P'_E(NZ-1)$$

Then for levels  $k = NZ-2$  to  $1$ ,

- a. convert the mixing ratio precipitation rate to an areal density precipitation rate at level  $k+1$ ,

$$P_G(k+1) = P'_E(k+1) \cdot f_{air}(k+1) \cdot \Delta z(k+1)$$

$\Delta z(k+1)$  is the thickness of model layer  $k+1$ , i.e. the distance between the point mid-way between model levels  $k$  and  $k+1$  and that between levels  $k+1$  and  $k+2$

- b. determine the precipitation leaving level  $k+1$ ,

$$P_L(k+1) = P_R(k+1) + P_G(k+1)$$

- c. calculate the evaporation of rain drops  $E_v(k)$  using  $P_L(k+1)$  in expression (21),

d. convert the evaporation to an areal density rate, restricting it to no larger than the precipitation available,

$$E_v(k) = \min [E_r(k) \cdot f_{air}(k) \cdot \Delta z(k), P_r(k+1)]$$

e. determine the precipitation reaching level  $k$

$$P_r(k) = P_r(k+1) - E_v(k)$$

f. and then enhance the precipitation generated at level  $k$  by accretion with rain drops reaching this level.

$$P_t(k) = P_t'(k) \left\{ 1 + \tilde{\alpha}_a P_r(k) / \tilde{c}_q \right\}$$

Finally negligible evaporation is assumed between the surface and the first model level (at a height of 10 m in the experimental version) to obtain the surface precipitation rate.

$$P_{r(surf)} = P_r(1) + P_t(1) \cdot f_{air}(1) \cdot \Delta z(1)$$

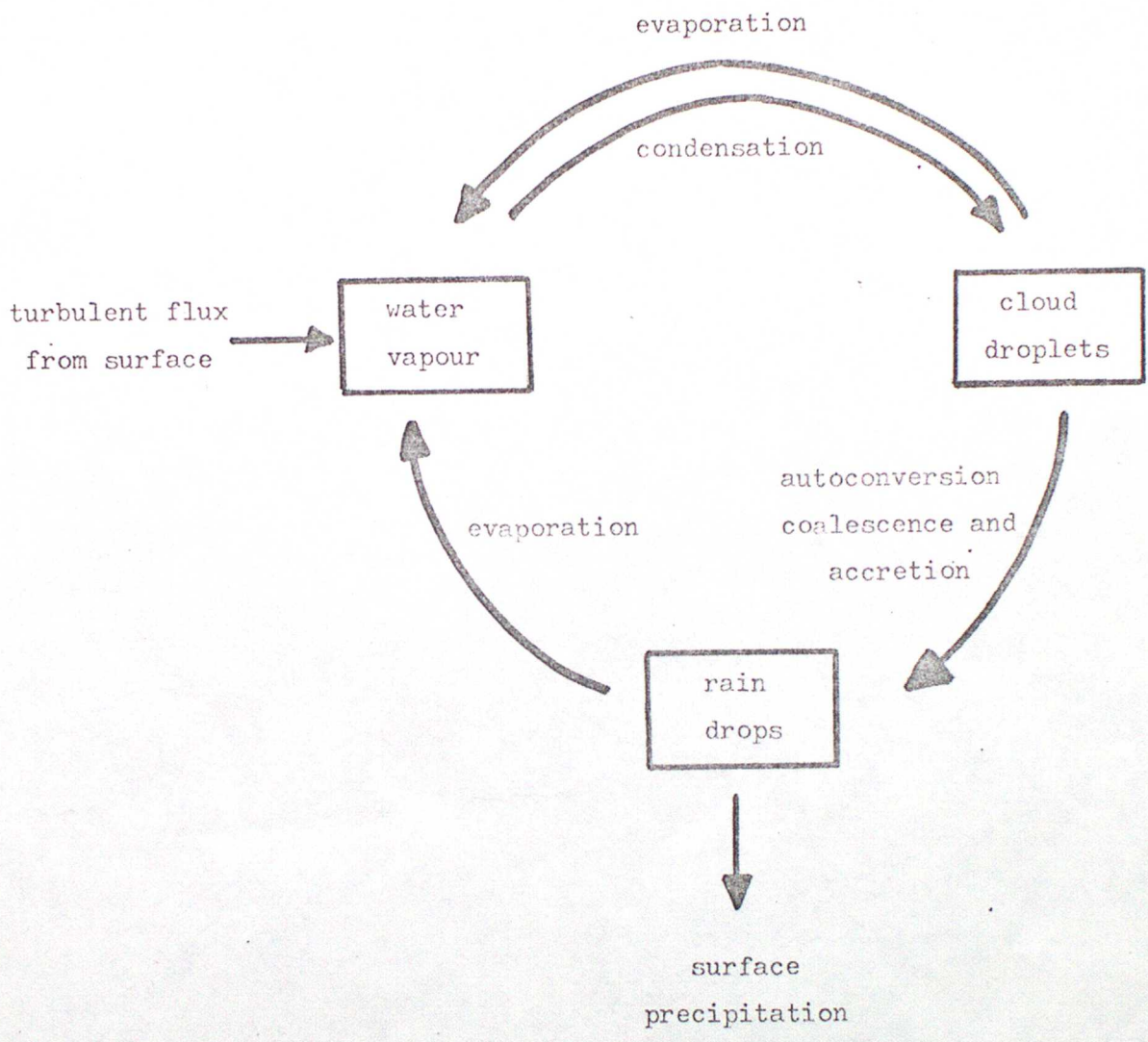


Figure 1. Processes represented in the stratiform condensation scheme

2 HRS

WIND VECTORS  
LEVEL 1 HEIGHT = 10M DATA TIME 18Z 5/1/1978 FCST TIME 120 X 60 SECS CLOUDY

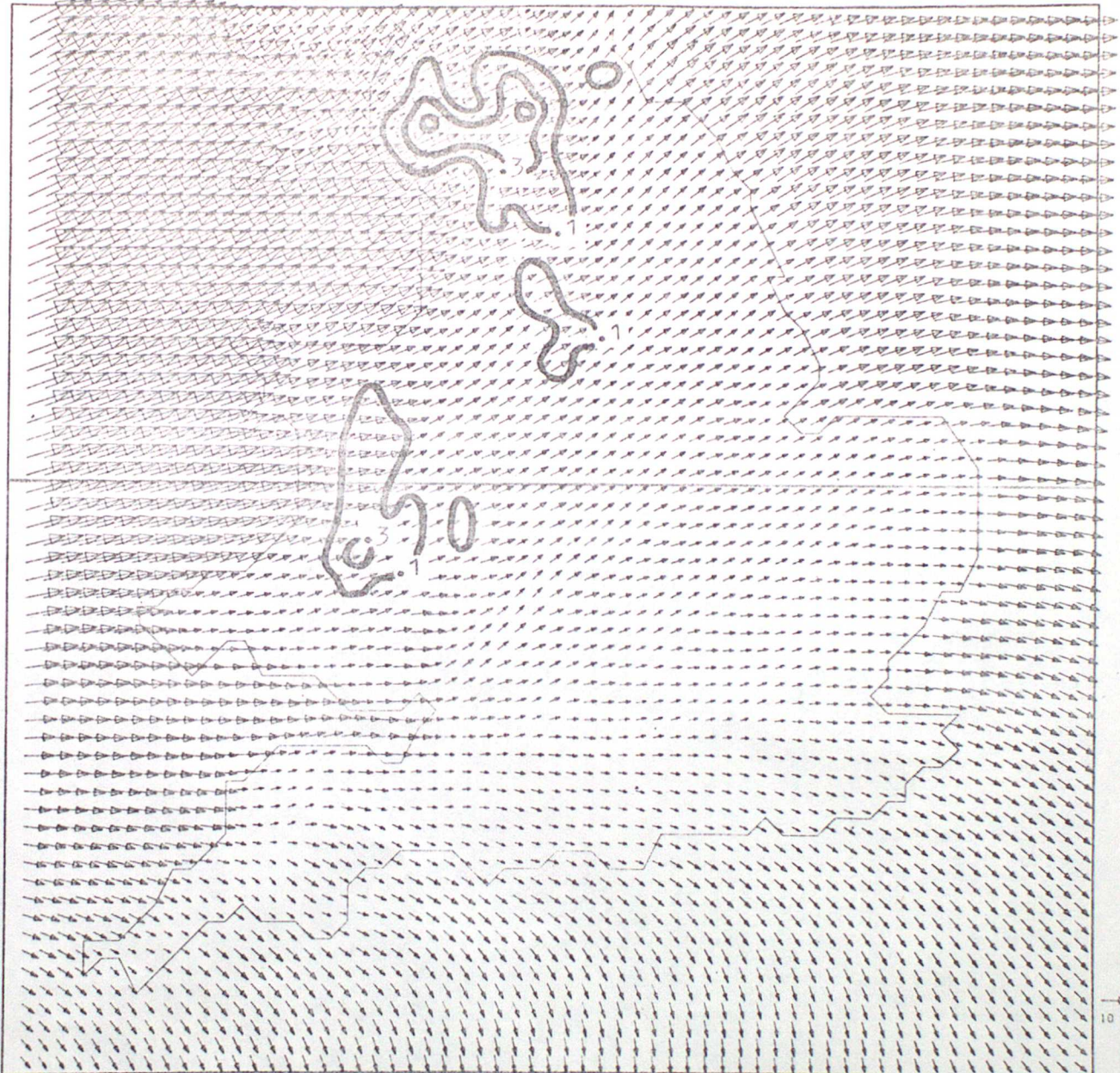


Figure 2. Cloudy forecast with surface precipitation ( $\text{mm hr}^{-1}$ )

POTENTIAL TEMPERATURE AND WIND VECTORS.

2 HRS

SECTION ALONG ROW 28

DATA TIME=18Z 3/1/1978

FCST TIME=120 X 60 SECS

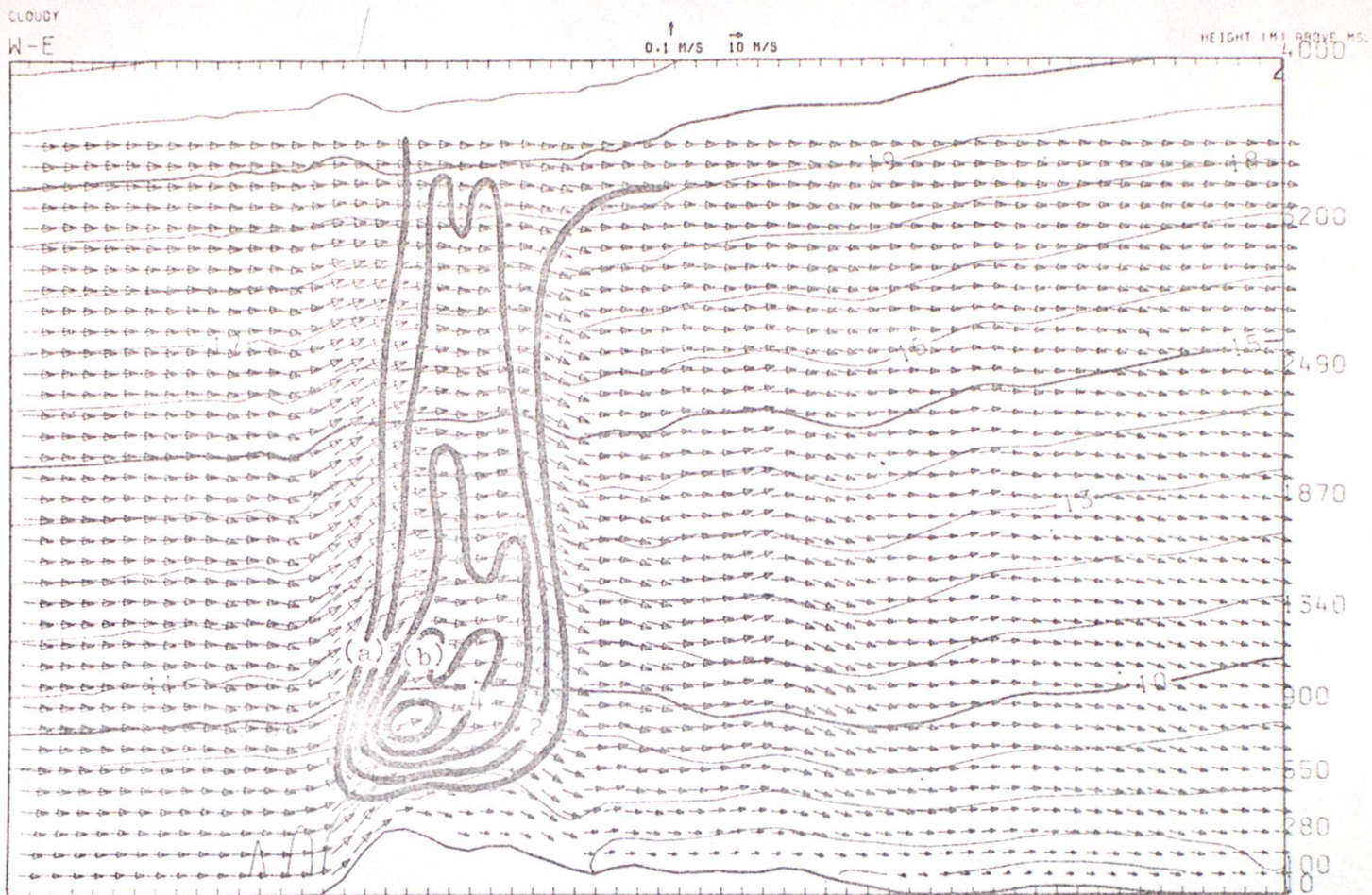


Figure 3. Cloudy forecast with cloud water mixing ratio ( $10^{-4}$ )

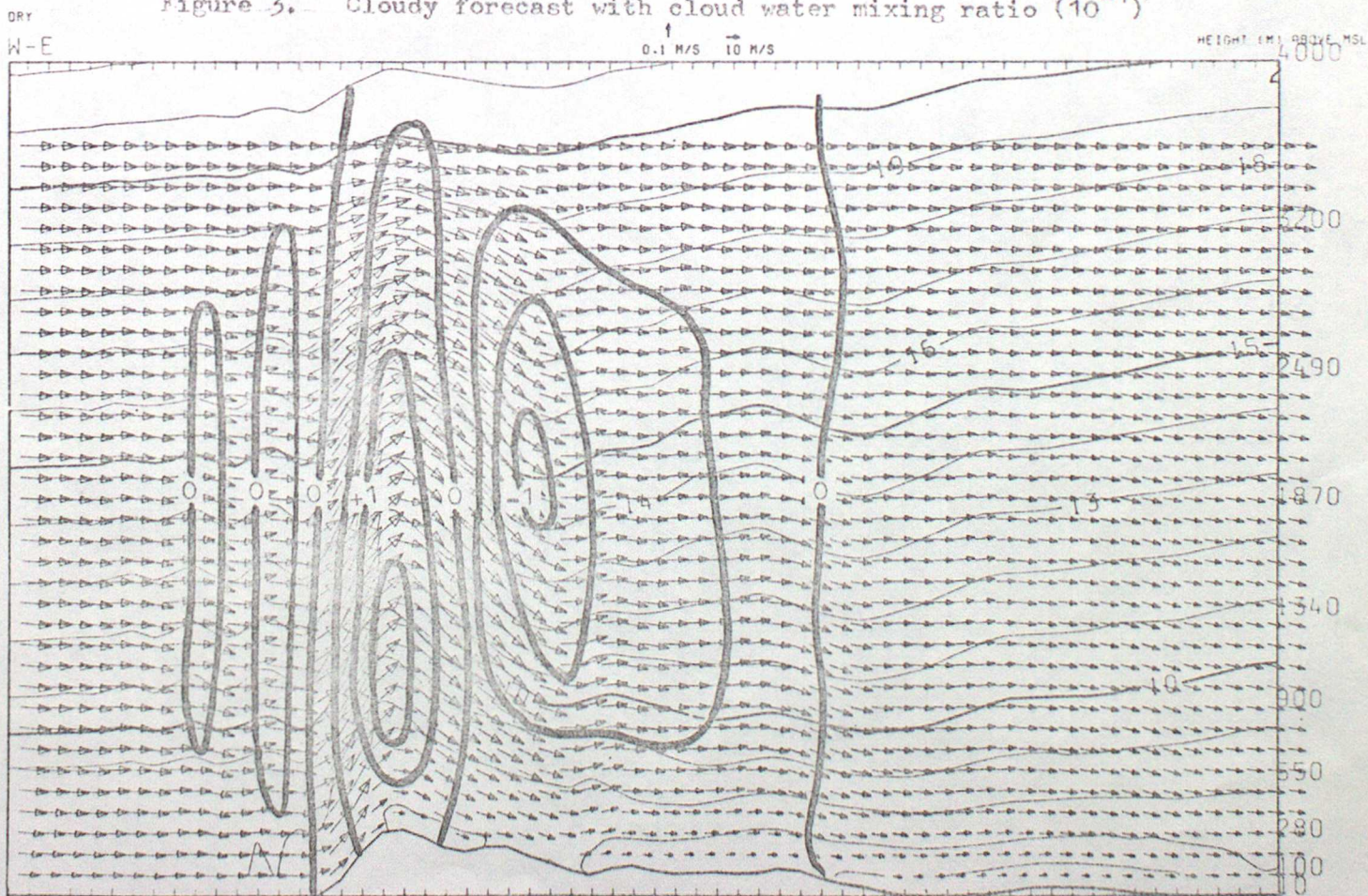


Figure 4. Dry forecast with potential temperature differences (K)

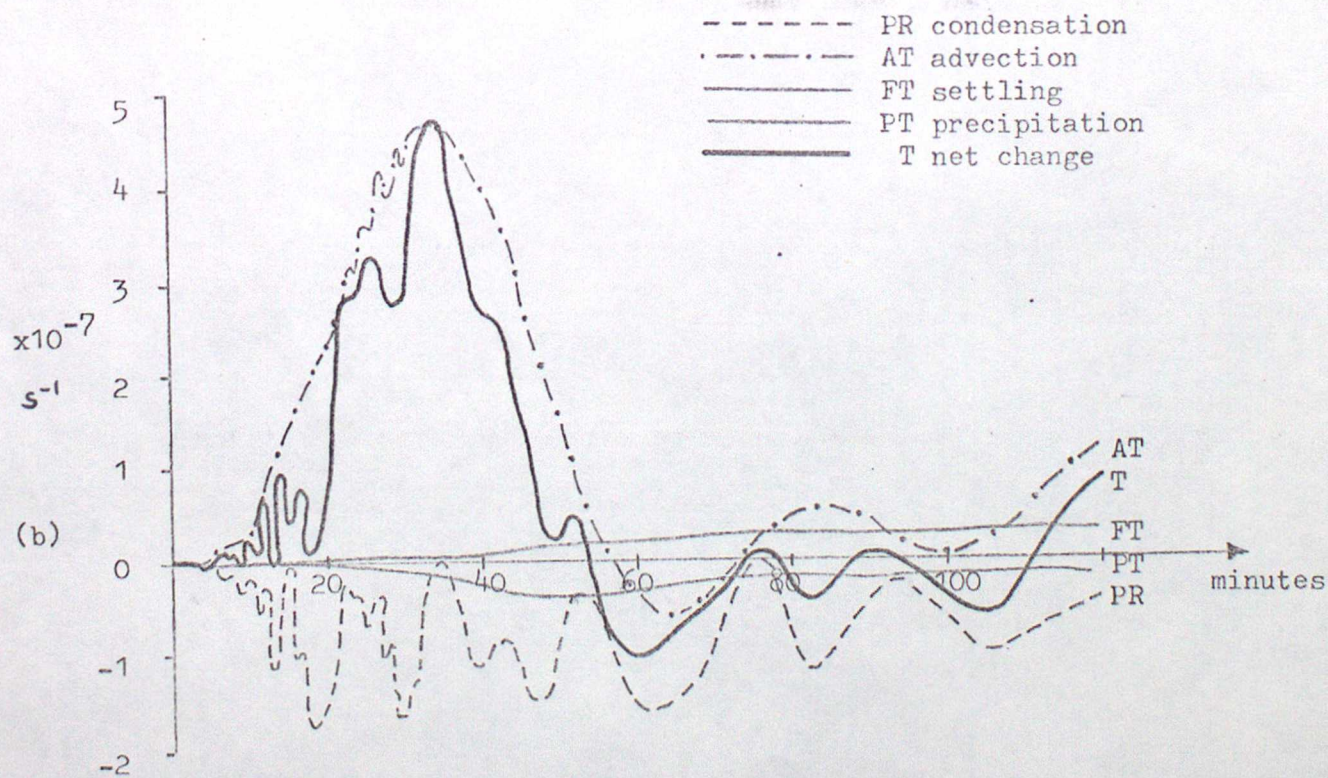
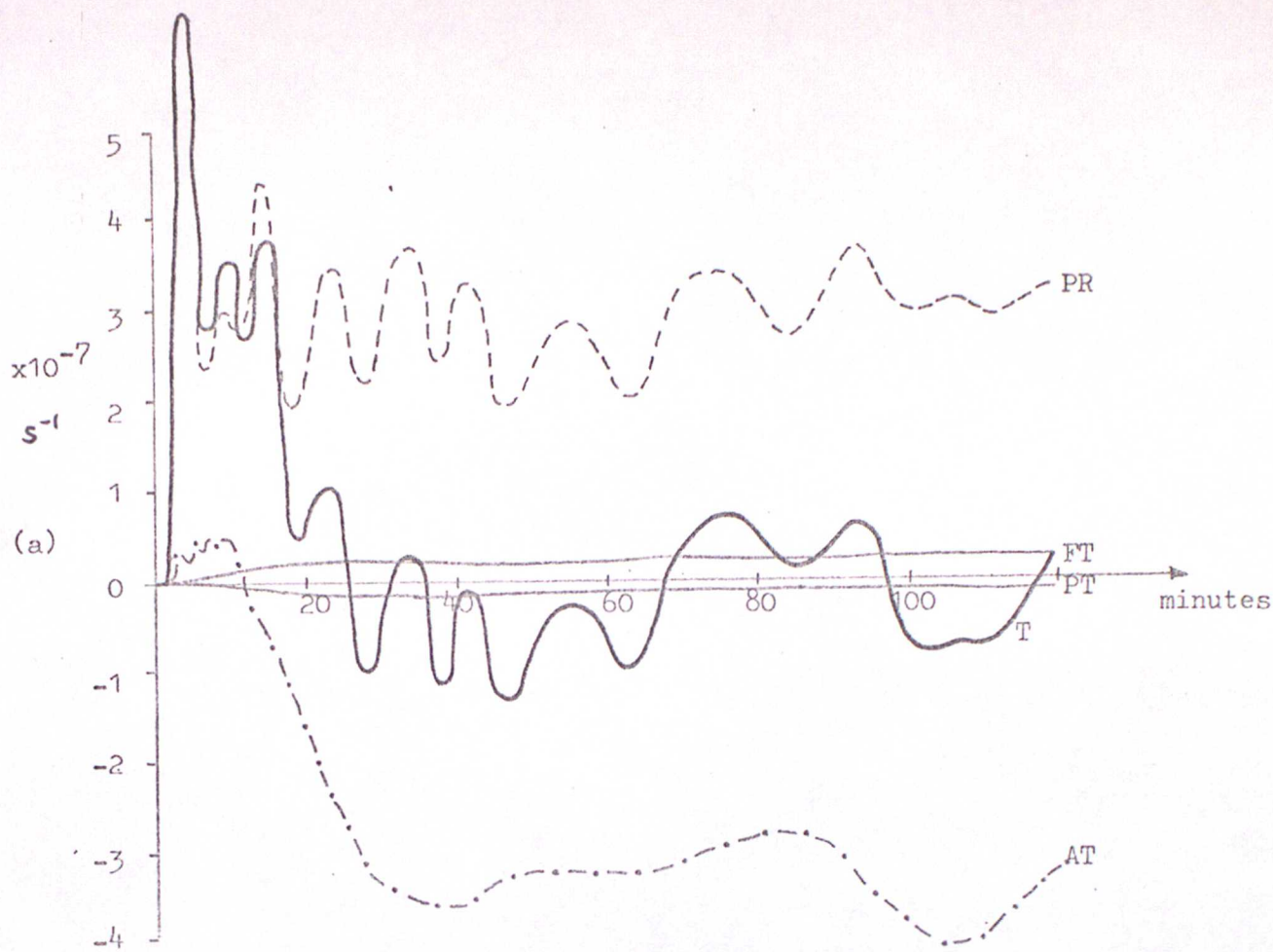
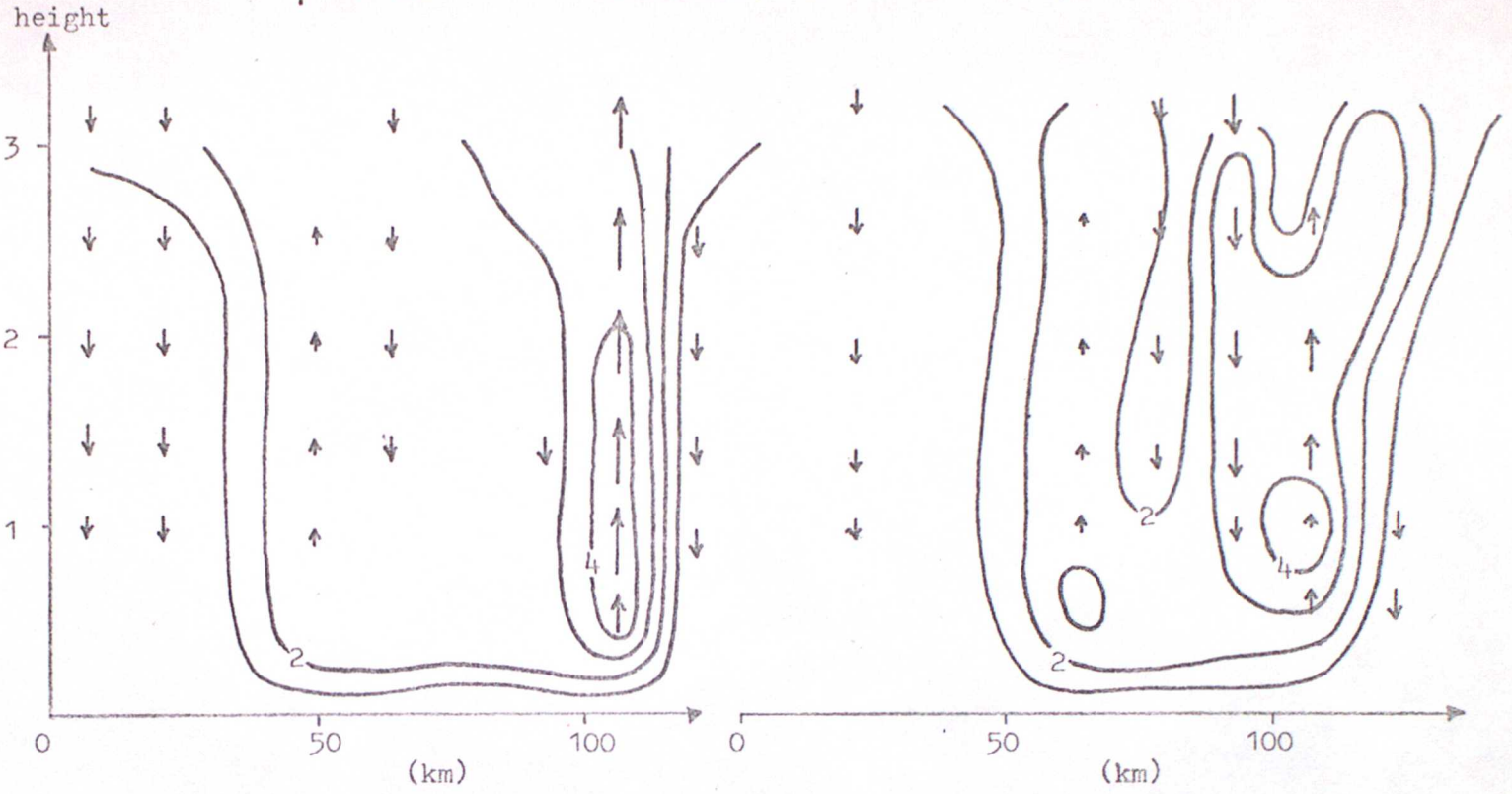


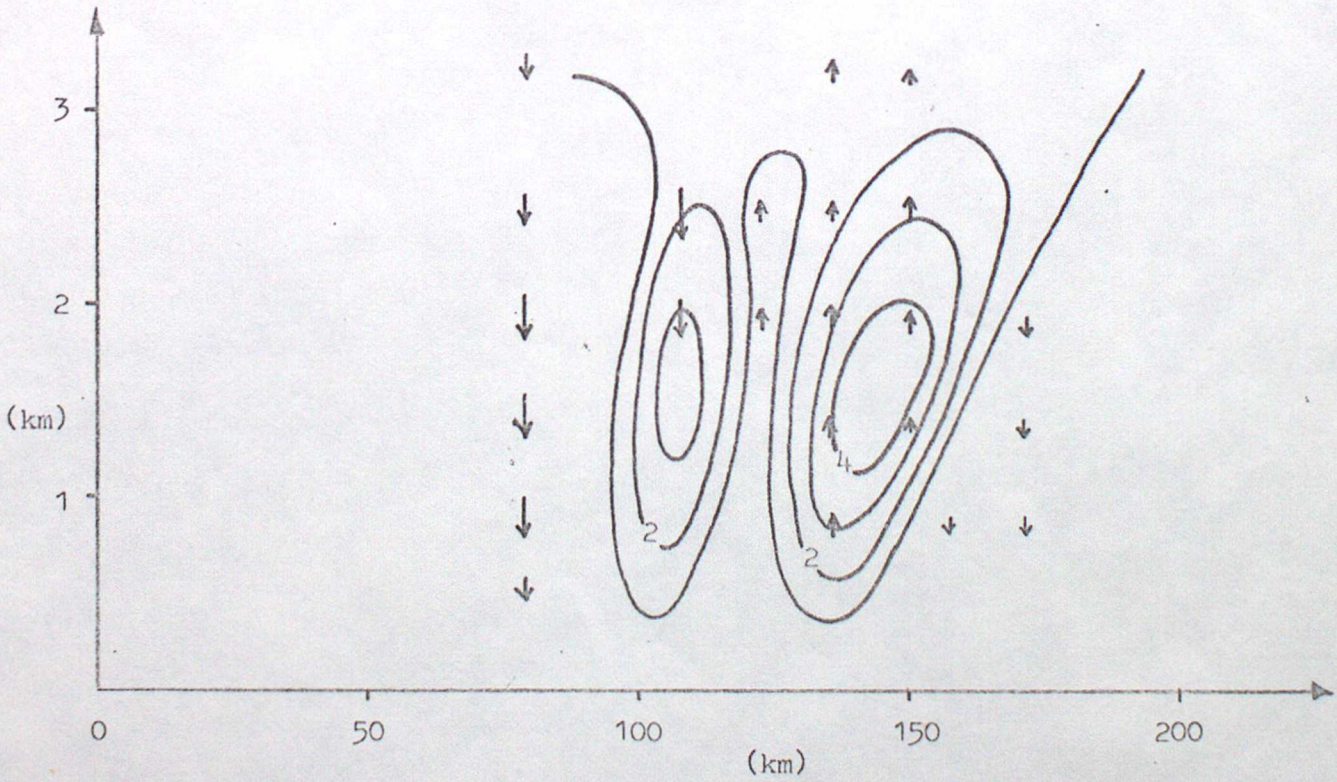
Figure 5. Cloud water budgets at (a) windward cloud edge  
 (b) 30km downwind (see Figure 3)

↑ 10 cms<sup>-1</sup> horizontal wind →



(a) End of assimilation period

(b) 20 timesteps after assimilation



(c) 80 timesteps after assimilation

Figure 6. Cross-sections of cloud water ( $\times 10^{-4}$ ) and vertical velocity for the assimilation experiment